



ELSEVIER

Palaeogeography, Palaeoclimatology, Palaeoecology 179 (2002) 19–41

PALAEO

www.elsevier.com/locate/palaeo

Reconstruction of mid-Cenomanian orbitally forced palaeoenvironmental changes based on calcareous dinoflagellate cysts

Jens Wendler*, Kai-Uwe Gräfe, Helmut Willems

Fachbereich 5, Geowissenschaften, Universität Bremen, P.O. Box 330440, 28334 Bremen, Germany

Received 24 November 2000; accepted 29 August 2001

Abstract

Mid-Cenomanian, precession-controlled (21 ka) chalk–marl couplets of the Cap Blanc Nez section (Anglo–Paris Basin) have been studied with focus on the effects which Milankovitch cycles have had on the palaeoenvironment. In this paper, we present micropalaeontological and lithological proxies that enable the reconstruction of both the cycle architecture and the transformation of the orbitally forced signal into the sediment. A palaeoecological reconstruction based on changes in calcareous dinoflagellate cysts (c-dinocysts) assemblages was carried out, in which two characteristic ecological assemblages of c-dinocysts were identified. Gradual changes in absolute and relative abundance of the cyst species in these assemblages over several couplets depict a bundling pattern which is interpreted to reflect the modulation of the intensity of the precession cycle by the eccentricity cycle (100 ka). The stacking pattern in the natural gamma ray signal and the carbonate and TOC content has the same period and provides lithological support of the bundling. A shelf basin circulation model is proposed to explain the relation between orbitally forced climate change, its palaeoenvironmental consequences and the resulting sedimentary cyclicality. Variations in surface water circulation are reflected in the sediment by the chalk–marl couplets, the most distinctive couplets occurring at the base and top of the bundles. While the chalks reflect well-mixed surface water conditions, the marls, particularly those at the bundle boundaries, can be interpreted as the sedimentary expression of stratified water masses. During deposition of these marls, reduced oceanic mixing due to low seasonality during strong precession maxima at the eccentricity maxima caused periods of water column stratification that in turn led to nutrient depletion and decreased productivity in the surface water masses. © 2002 Elsevier Science B.V. All rights reserved.

Keywords: Cretaceous; Cenomanian; Milankovitch cycles; palaeoceanography; calcareous dinoflagellate cysts; gamma ray

1. Introduction

Chalk–marl couplets of the Cenomanian of the Anglo–Paris Basin are characterised by a more or

less distinct light/dark cyclicality. These couplets have been interpreted as orbitally forced sedimentary cycles (e.g. Fischer and Schwarzscher, 1984; Bottjer et al., 1986; Gale, 1990, 1995; Schwarzscher, 1993, 1994; Mitchell and Carr, 1998). They are thought to represent the 21-ka precession signal, an interpretation which is supported by (i) correlation with the radiometric dat-

* Corresponding author. Fax: +49-421-2184451.
E-mail address: wendler@uni-bremen.de (J. Wendler).

ing of the Cenomanian stage based on bentonite bearing sections of the Western Interior Basin (Obradovich, 1994), and (ii) spectral analysis (Gale, 1990, 1995; Gale et al., 1999).

The amplitude of the precession signal is modified in amplitude by the 100-ka eccentricity cycle, which leads to an approximate 5:1 bundling of couplets and provides the most conspicuous evidence for the orbital forcing of sedimentary cycles (House, 1995). Such bundling of couplets can, for example, clearly be recognised in the Barremian of the Gubbio section, Italy (Schwarzacher, 1993), where strong variations in grey scale, carbonate content and bed thickness follow the above-mentioned 5:1 ratio. However, the superimposition of precession and eccentricity cycles is often preserved in the sediment as rather subtle changes that cannot be detected in the field. In the couplet succession of the Anglo–Paris Basin, bundling is difficult to prove without the confirmation by microscopic investigations. The current high-resolution micropalaeontological analysis, however, provides an objective measure to recognise this cyclicity.

The main tool used in the present study of the Anglo–Paris Basin couplet succession is the qualitative and quantitative analysis of their calcareous dinoflagellate cyst (*c*-dinocyst) content. *C*-dinocysts are formed during the life cycle of the Calciodinelloideae, a subfamily of the dinoflagellates (Fensome et al., 1993). *C*-dinocysts have been commonly described as ‘calcispheres’ in the fossil record, without a further distinction of species. Although most of them do not show any signs of paratabulation, some species do reflect the peridinioid plate pattern of the corresponding motile dinoflagellates very clearly. We know from recent species that the Calciodinelloideae are unicellular, autotrophic, primary producers that live in the upper water column. As such, they can play an important role in reconstructing climatically induced oceanic changes. *C*-dinocysts form one of the three major components of the investigated carbonate, which is almost entirely of biogenic origin. The mean Coccoliths:foraminifera:*c*-dinocysts ratio is about 70:20:5 (%), these three groups forming 95% of the biogenic components of the investigated material.

Our study of *c*-dinocysts distinguished to the species level is the first to apply them for the interpretation of Cenomanian sedimentary cycles and their stacking patterns. Climatic changes resulting from orbital forcing are reflected in the sediment, as they strongly influence the biogenic (carbonate, organic matter) and abiogenic (siliciclastic) sedimentation. Changes in abundances and distribution of the biogenic components can be caused primarily by variations of environmental parameters, such as surface water temperature, stratification of the water column and nutrient input. Secondly, diagenesis may have altered the sedimentary distribution of biogenic and abiogenic components but is not considered to have obscured the primary cyclic changes in the investigated section (e.g. R.O.C.C. group, 1986). Diagenetic bedding in the sense of Ricken (1986) can be excluded due to the presence of primary sedimentary features, in particular burrows that cross marl–chalk contacts. However, differences in cementation between chalks and marls point at some late diagenetic enhancement of the rhythmic bedding (Kennedy, 1967).

Here, an approach is made to reconstruct the palaeoceanographic response to variations in orbital parameters through the integrated interpretation of palaeontological and lithological data.

2. Materials and methods

2.1. Regional geology

We investigated a 14-m long sedimentary succession in the mid-Cenomanian of the Cap Blanc Nez section near Escalles/SW of Calais, France (Figs. 1 and 2). The 78-m thick profile of the Cenomanian is the reference section for this part of the Anglo–Paris Basin (Robaszynski and Amédro, 1993). It represents a central basinal, outer shelf position (Fig. 1), characterised by a continuous deposition of 12 to 110 cm thick chalk/marl alternations. These carbonate sequences were deposited at water depths between 300 m and 500 m (Hart, 1980; Gräfe, 1999), well below the storm-wave base. Palaeogeographically, the investigated section was positioned at around 40° N, i.e. at

mid northern latitudes (Ziegler, 1990; Voigt, 1996).

During the Cenomanian and Turonian, a continuous sea level rise led to the world-wide expansion of shelf seas (Haq et al., 1987). Several seaways enabled a connection between the Boreal and Tethyan Realms since the Early Cretaceous. Both Tethyan and Boreal influence can, therefore, be expected in the investigated area. The interfingering of these two water masses was thought to be expressed in the lithofacies; Tethyan deposits being carbonate-rich and Boreal sediments characterised by high proportions of clay (Keupp, 1993; Mutterlose, 1989; Mutterlose and Ruffell, 1999).

Tectonic activity of the main structural elements near the Escalles section was relatively calm during most of the Cenomanian (Ziegler, 1975; Ziegler, 1990). Tuffs are not present in the investigated section part. Thus, no major disturbances of the sedimentation occurred and reworking, tectonically induced movement or intercalation of volcanogenic sediments did not disturb the continuous sedimentation.

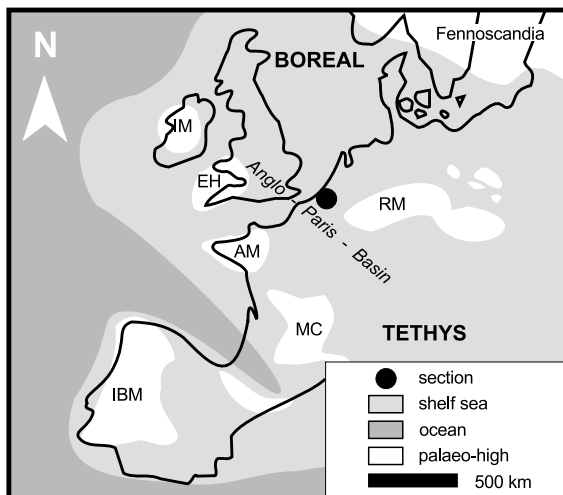


Fig. 1. Palaeogeography of western Europe during the Middle Cenomanian (after Ziegler, 1990); AM = American Massive, EH = English High, IBM = Iberian Massive, IM = Irish Massive, MC = Massive Centrale, RM = Rheinish Massive.

2.2. Material

Three main lithofacies types can be distinguished in the studied interval (Gräfe, 1999): (i) grey to white chalk (light-coloured), (ii) marly grey chalk (light-coloured); and (iii) grey marlstone (dark-coloured). It should be kept in mind that the generally used term 'marl' for dark layers is lithologically misleading because of their high carbonate content. Bio-, litho- and sequence-stratigraphy according to Robaszynski and Amédéo (1993), Robaszynski et al. (1998) and Owen (1996) are summarised in Fig. 2.

We investigated the part of the section ranging from 42.3–56.5 m above the base of the Cenomanian (Fig. 2). Two parts within this succession, termed EscA (Escalles A) and EscB, were analysed for stacking patterns of the couplet succession using various parameters. EscA, covering the interval from 42.3 to 46.5 m, is positioned in the *Acanthoceras rhotomagense* ammonite zone, its base forming the transition from the *Turrilites costatus* to the *Turrilites acutus* ammonite sub-zone. It represents the lower half of lithostratigraphic member I21 of Robaszynski and Amédéo (1993) and is in the range of couplets > C20 of the couplet numbering scheme of Gale (1990) (Highstand Systems Tract (HST) of sequence 3). EscB, covering the interval from 53.8 m to 56.5 m, is a set of couplets in the lower *Acanthoceras jukesbrownei* ammonite zone, within lithostratigraphic members I22 and I23, and couplets D1–D5 (lower Transgressive Systems Tract (TST) of sequence 4) according to the subdivisions of Robaszynski et al. (1998) and Gale (1995), respectively.

2.3. Methods

35 samples from EscA and 25 samples from EscB were analysed for their c-dinocyst content, grain size distribution, carbonate content, total organic carbon (TOC) content and natural gamma ray at a sample spacing of 10 cm. To connect the two parts of the section, additional samples with 20–100 cm sample spacing were studied between the sections with focus on the marls.

All microscopic investigations on microfossils

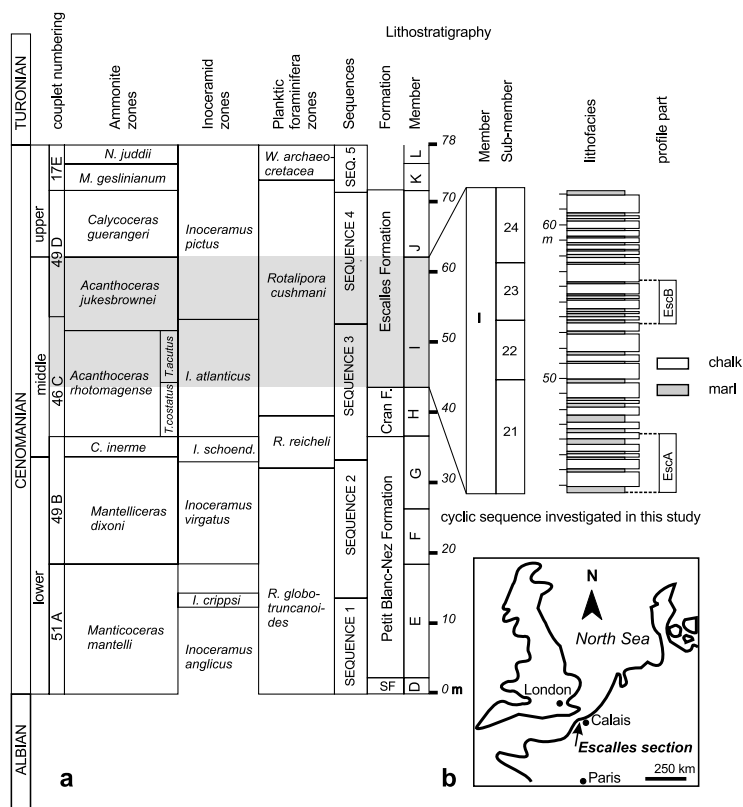


Fig. 2. (a) Integrated illustration of the bio-, sequence- and lithostratigraphy of the investigated section (modified after Robaszynski and Amédro, 1993; Gräfe, 1999). Sequence and couplet numbering after Gale (1995); scales in meters from base of Cenomanian. Abbreviations: C – *Cunigniticeras*, M – *Metoicoceras*, N – *Neocardioceras*, W – *Whiteinella*. (b) Geographic location of the investigated section (arrow).

and non-carbonate grains were carried out using disintegrated material. Sample sizes of approximately 0.5 g were processed using repeated freezing and thawing in sodium–sulphate solution. The disintegrated samples were sieved into three fractions (< 20 μm , 20–75 μm and > 75 μm). The two coarse fractions were weighted to obtain information on the grain size distribution.

The micropalaeontological analyses comprise

investigation of absolute cyst abundances, relative abundances and ratios between cyst species. Absolute abundances are given in cysts/mg of the 20–75- μm fraction. Mean cyst sizes of the species *Pithonella sphaerica* were measured on about 50 randomly picked specimens per sample for a 2-m interval spanning the basal two marl–chalk couplets of EscA. In addition to the cyst data, sizes of foraminifera of the 20–75- μm size fraction were

Plate I. Calcareous dinoflagellate cysts used in the quantitative analysis; scale bar is 10 μm .

Pithonella sphaerica

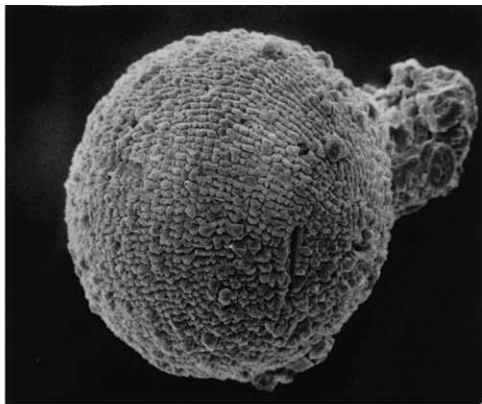
Pithonella ovalis

Pithonella discoidea

Pirumella sp.

Cubodinellum renei

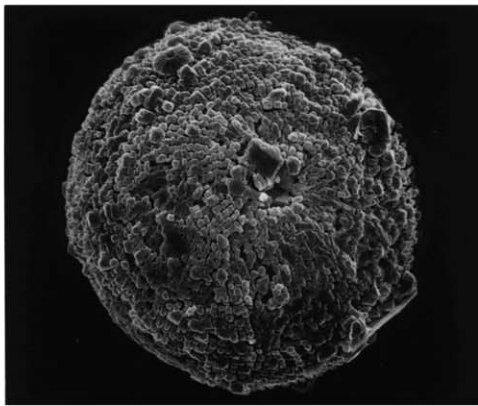
Pentadinellum vimineum; apical view



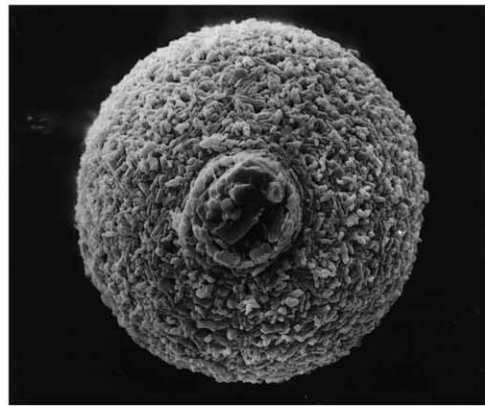
1



2



3



4



5



6

measured under the scanning electron microscope (SEM; 50 tests per sample and four samples within EscA).

In order to produce quantitative c-dinocyst data, a weighted microsplit of 1–4 mg of the 20–75- μm grain size fraction was taken by measuring the weight of the entire fraction before and after splitting. The complete microsplit was counted using a Zeiss binocular microscope Stemi2000 with magnifications ranging from 80 \times to 120 \times . Specimens which could not be taxonomically specified by their light-optical characteristics were picked and studied with the SEM.

In order to obtain a detailed lithological log of the investigated section, the natural gamma ray signal measured in the field was analysed. Gamma ray and the carbonate content of the marls were cross-plotted to characterise the marl types. The carbonate content and TOC content were determined using LECO measurement.

For the interpretation of the gamma ray data, an analysis of the clay mineralogy was necessary. Six samples at an approximate sample spacing of 1.5 m, covering two major oscillations of the gamma

ray log, were chosen. The variations of the clay content within couplets of several Anglo-Paris Basin sections were analysed by Ditchfield (1990), so we focused on variations between marl types only. The samples were decarbonised with a 10% EDTA (Titriplex III) solution which was buffered with NaOH to pH \sim 8, at 50°C under continuous stirring for 3 days. The XRD-analysis was performed with a diffractometer D500 on a smear slide containing the <2 μm fraction.

An overview of the c-dinocyst species studied here is given in the Appendix. All material is stored at the Division of Historical Geology and Palaeontology, University of Bremen, Bremen, Germany.

3. Results

3.1. Micropalaeontology

3.1.1. Absolute and relative abundances

The quantitative method applied in this study focuses on the six most abundant c-dinocyst spe-

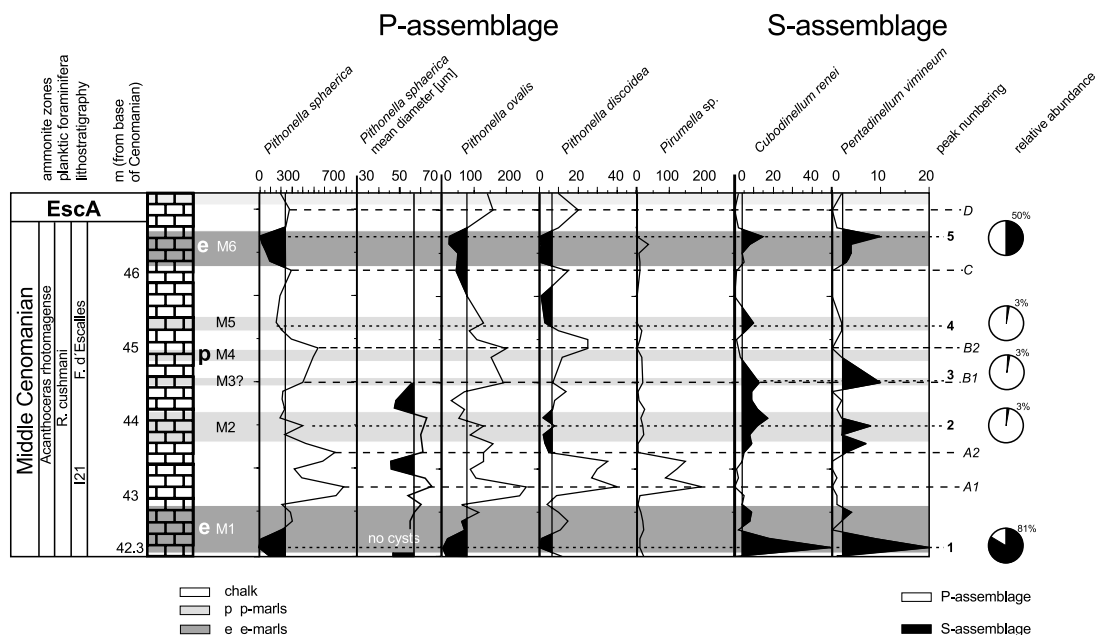


Fig. 3. C-dinocyst absolute abundances (cysts/mg of the 20–75- μm size fraction) in section EscA. P-assemblage: positive peaks relative to mean value (solid vertical lines) are white and are marked with a letter; negative peaks relative to mean value are black and marked with a number. These correlate with excursions (black) of the S- assemblage. For lithological data, see Fig. 6.

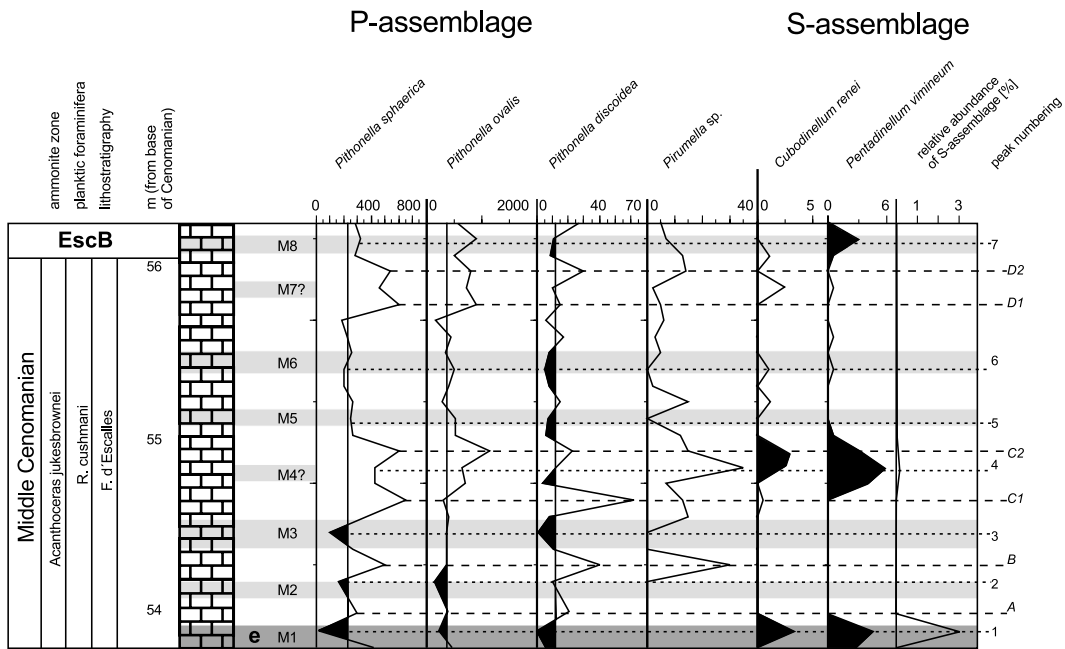


Fig. 4. C-dinocyst absolute abundances (cysts/mg of the 20–75- μ m size fraction) in section EscB. P-assemblage: positive peaks relative to mean value are white and are marked with a letter negative peaks relative to mean value are black and marked with a number. These correlate with excursions (black) of the S-assemblage.

cies (Appendix; Plate I) which are common throughout the section: *Pittonella sphaerica*, *Pittonella ovalis*, *Pittonella discoidea*, *Pirumella sp.*, *Cubodinium renei*, *Pentadinellum vimineum*.

All cyst species mentioned above are generally present in chalks as well as in marls. Changes in absolute and relative abundance can be noted between these lithofacies and, in form of subtle variations, also within the lithotypes. Marls typically show low absolute abundances and a diverse c-dinocyst association due to the presence of rare species (listed in the Appendix). In intervals of high carbonate content (i.e. chalks), high abundances and low diversity are typical.

Two assemblages of c-dinocysts can be distinguished due to the cyst distribution patterns: (i) the P-assemblage (P = Pittonelloideae), which consists predominantly of Pittonelloideae (>95%) and *Pirumella sp.*; and (ii) the S-assemblage (S = Sculptured/paratabulated), which contains the paratabulated species *Cubodinium renei* and *Pentadinellum vimineum* that may represent up to 80% of the c-dinocyst association (Figs. 3,

4 and 9). These two assemblages show an inverse absolute abundance pattern (Figs. 3 and 4). In marls, distinct and often sharp-cut peaks in absolute abundances (cysts/mg) of the S-assemblage (black, numbered peaks) coincide with very low abundances of the P-assemblage. In contrast, broad maxima in abundance are characteristic of the P-assemblage (white, lettered peaks), and are commonly positioned in chalks where S-assemblage abundances are low. A major peak of *Pirumella sp.* (Fig. 3, peak A1/A2) is correlated with such a broad peak, thereby including this species into the P-assemblage.

Although the above-mentioned relation between c-dinocyst assemblages and the lithotypes is quite characteristic, the relation of the two groups varies between the chalk-marl couplets. This allows the differentiation between different marl types, which plays a key role in the further analysis of the cyclic pattern. The most distinct marl type is characterised by an almost pure S-assemblage, while Pittonelloideae abundances may decrease to near absence (Figs. 3, 4 and 9).

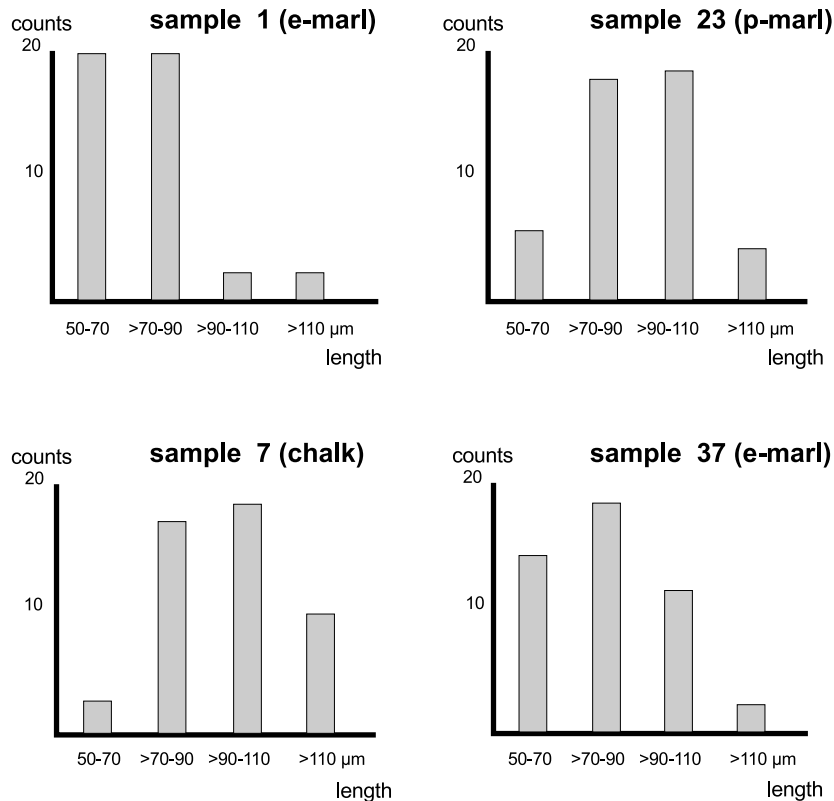


Fig. 5. Length distribution of *Heterohelix moremani* in four samples of the couplet bundle EscA. Note the dominance of smaller specimens in e-marls.

A significant feature is the sharpness of the positive abundance excursions of species of the S-assembly, such as peaks 1 and 5 in EscA (Fig. 3). The total number of c-dinocysts is low in these beds. Marls of this type will be termed ‘event-marls’ (e-marls) here, because they appear as short-term, exceptional events. The opposite to the e-marls are the so-called p-marls (= Pithonelloideae-rich marl). Relatively high abundances of Pithonelloideae (comparable to chalks) are characteristic for these marls (for example M3(?) and M4 in Fig. 3), while the S-assembly may be present in low numbers or even absent.

Besides their distinct c-dinocyst association, e-marls are characterised by partial solution of foraminifera and an increased number of very small foraminifera in the 20–75-μm fraction (Fig. 5). Among these small species, the planktic foraminifer *Heterohelix moremani* Cushman is a common

form. The length of tests of *H. moremani* was measured in the two e-marls, the p-marl and a chalk of EscA with focus on specimens with not less than seven chambers (adult forms).

3.1.2. Variations within the dominant genus – the *Pithonella sphaerical*/*Pithonella ovalis* ratio (*Ps/Po*-ratio)

Pithonelloideae are the most abundant c-dinocyst species in the investigated material. The *Ps/Po*-ratio is a statistically powerful indicator of environmental change as these two species lived in different palaeoenvironments (e.g. Kaufmann, 1865; Bignot and Lezard, 1964; Bein and Reiss, 1976; Bouyx and Villain, 1986; Dali-Ressot, 1987; Zügel, 1994; Dias-Brito, 2000). In EscA the *Ps/Po*-ratio has a relatively constant mean value of 3 but shows distinct negative and positive excursions from this mean value which vary be-

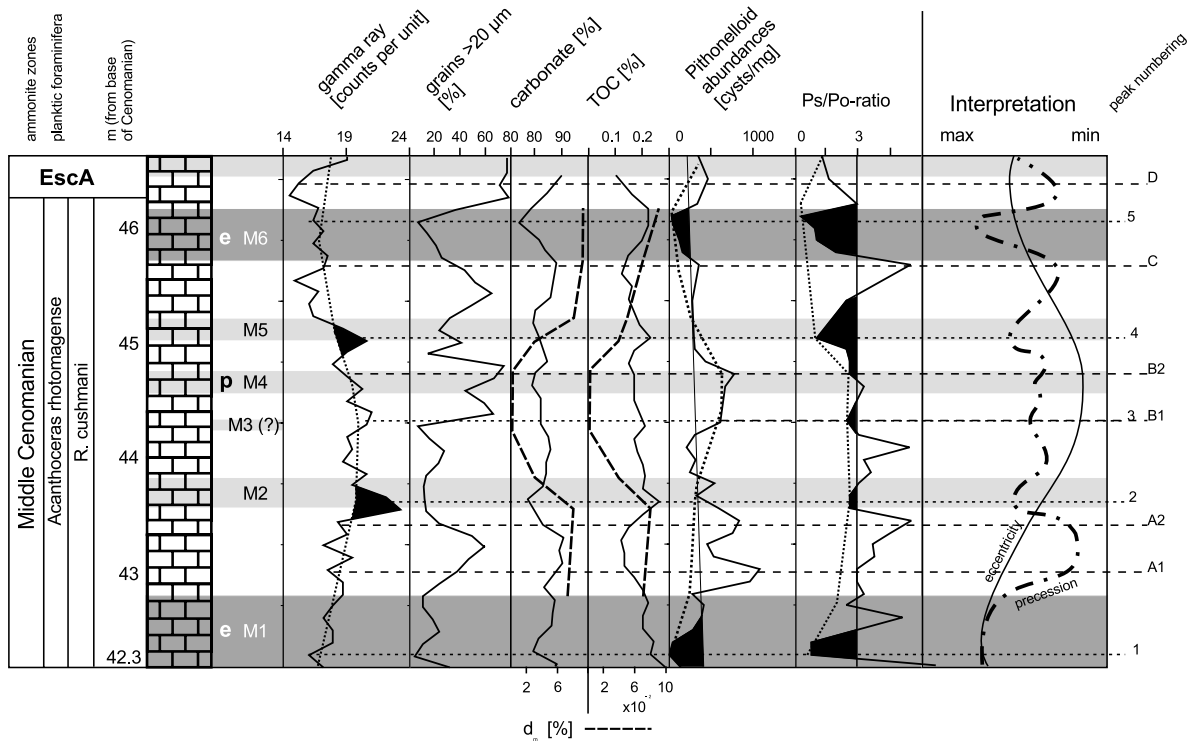


Fig. 6. Relations between lithological data and P-assemblage data of section EscA. Dotted curves=low-frequency curves of values in the marls; d_m = difference in mean percentage between marl and adjacent chalk. Interpretation = reconstructed Milankovitch cyclicity reflected in the data. Peak numbering and lithological signature as in Fig. 3.

tween almost 0 and 6 (Fig. 6). In EscB, the mean value drops to 0.6 but the Ps/Po-ratio still fluctuates significantly between values of 0 and 2 (Fig. 7).

In the studied material, a low Ps/Po-ratio is always the result of a stronger decrease in abundance of *Pithonella sphaerica* relative to *P. ovalis*. This is characteristic for the marls and corresponds with generally decreased Pithonelloideae abundances. There is a gradual variation in Ps/Po values between marls (low-frequency curve in Fig. 6), with lowest Ps/Po values observed in the e-marls. The ratio stays close to the mean value around the p-marls. Thus, the distinction of marl types on the basis of cyst association changes as discussed in Section 3.1.1 is supported by the Ps/Po-ratio.

Contrary to the marls, chalks are generally characterised by a high Ps/Po-ratio due to an increase in abundance of *Pithonella sphaerica* rela-

tive to *P. ovalis*. A significant minimum in the size of specimens of *P. sphaerica* occurs within the basal chalk of EscA, which was analysed for morphometric changes (Fig. 3). This minimum is accompanied by a simultaneous decrease in abundances of Pithonelloideae, a peak of the Ps/Po-ratio, and a particularly high carbonate content (Fig. 6).

3.1.3. Cycle architecture of EscA compared to EscB

A systematic succession of marl types is present in EscA (Figs. 3 and 6). M1 and M6 are e-marls whereas M2 and M5 are less distinctive marls. Towards the middle of this section, differences between chalks and marls concerning the relation between the P- and S-assemblages and the Ps/Po-ratio are least developed. An interference between the S-assemblage and the P-assemblage is characteristic of this interval (p-marls M3(?) and M4).

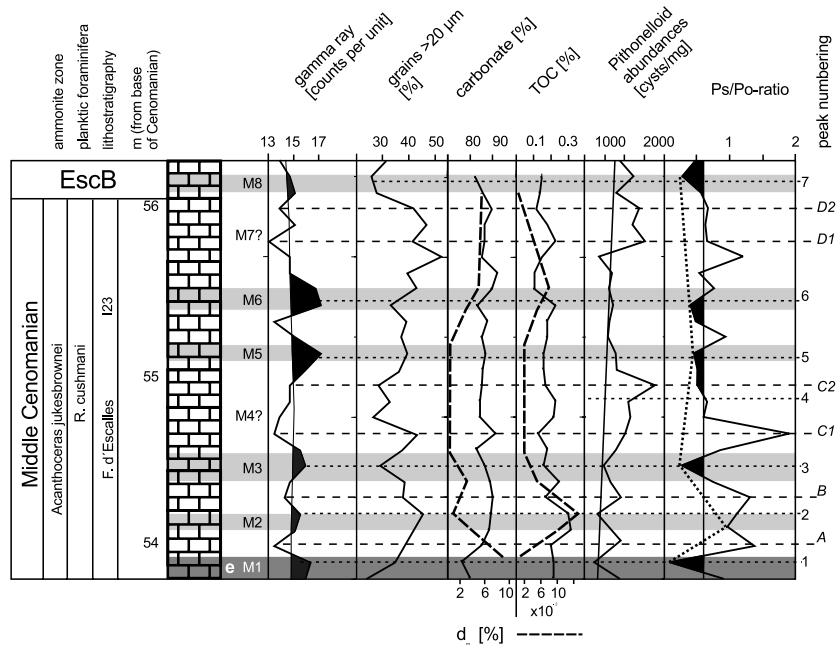


Fig. 7. Relations between lithological data and P-assemblage data of section EscB. Dotted curves – low-frequency curve between values in the marls; d_m – difference in mean percentage between marl and adjacent chalk. Couplet succession of EscB enables no interpretation as in EscA. Peak numbering and lithological signature as in Fig. 4.

The resulting pattern is a bundling of five couplets, bounded by e-marls. From the base towards the top of this bundle, the abundance patterns of the c-dinocyst assemblages gradually oscillate from the event-marl situation to the p-marl situation in the middle of the bundle, and then back to the next e-marl situation.

The c-dinocyst abundances of EscB are shown in Fig. 4. The abundances of the species of the S-assemblage are lower than in EscA, leading to a lower resolution of this parameter. Whereas in EscA, all numbered peaks (in the marls) were correlatable between the P- and S-assemblage, only peak 1 can be correlated between the two assemblages in EscB. Double peaks are characteristic of the thickest chalk layers in EscB and EscA. A near-symmetric cycle architecture, as is present in EscA, cannot be reconstructed in EscB, as only e-marl M1 is unambiguous. No bundling of couplets can be reconstructed from the low-frequency curves in Ps/Po-ratio and Pithonelloid abundances (Fig. 7).

3.2. Lithology

3.2.1. Gamma ray

The gamma ray data for EscA and EscB are shown in Figs. 6 and 7. The plot for the entire investigated section is given in Fig. 9. The gamma ray is a proxy for the clay content of sediments. High counts per unit (cpu) represent layers rich in radioactive elements (K, U or Th) which are mainly incorporated in clay minerals. Thus, large excursions generally occur in the marls, whereas chalks show low values caused by their higher carbonate/clay ratio. Due to the declining overall clay content from EscA to EscB, the gamma values continuously decrease throughout the entire section (Fig. 9; Gräfe 1999, Figs. 5 and 6).

Fig. 6 shows that a positive correlation exists between the low-frequency curve of the gamma ray log of marls and the Pithonelloideae distribution throughout EscA. This curve shows a gradual increase from low values in the e-marls (M1, M6) to higher values in between them. In EscB,

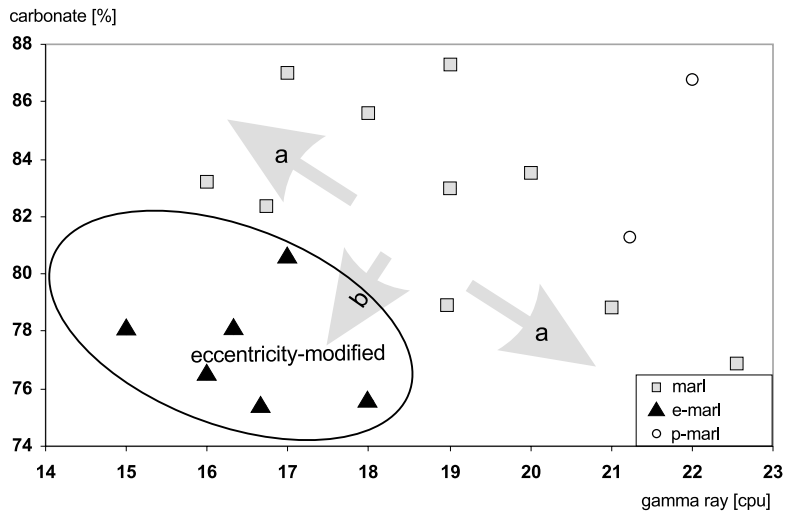


Fig. 8. Cross-plot of gamma ray data and carbonate content of the marls from EscA and bundle 2. Note the eccentricity-controlled shift (b) of e-marls compared to the normal relation (a).

only the gamma ray variations between chalks and marls can be recognised. Changes between marls, as in EscA, are not clearly reflected, probably since the lower overall gamma value leads to a lower resolution.

In Fig. 8, the gamma ray signature of marls is plotted against their carbonate content. The general trend from high carbonate content and low gamma ray values to low carbonate content and high gamma values is shifted in the e-marls to generally lower values of both parameters. This could be due to the composition of the clay mineral fraction. To test this hypothesis, we chose six samples from e-marls and p-marls (for sample positions see Fig. 9) and examined their relative content of kaolinite, chlorite and illite. Variations in the relative quantities of these clay minerals are on the order of 1% only. The half value width of illite, as a measure for the crystallinity, varies between 0.48 and 0.57 and can be regarded as constant.

The results reveal a stable clay association which varies very little between the samples (Fig. 9). Though the small variation in the illite/kaolinite-ratio seems to correlate positively with the gamma ray data in EscA, it fails to explain the gamma ray peak in the second p-marl analysed (Fig. 9). Additionally, it is not significant

enough to cause the changes in the gamma ray log. Besides clay minerals, a major source for elevated gamma ray values is uranium-binding organic matter (ten Veen and Postma, 1996). However, no relation between the TOC content and the low-frequency curve in the gamma ray log could be found (Figs. 6 and 7).

3.2.2. Grain size distribution

The percentage of grains with a size larger than 20 μm in EscA is clearly related to the light/dark lithological changes, chalks being coarser grained than marls (Fig. 6). This difference in grain size represents a clearer distinction between the light and dark layers than the carbonate content does. As the marls contain less grains with a size > 20 μm but still have a high carbonate content (see Section 3.2.3), the light/dark-cyclicity is to some extent a simple optical expression of these grain size changes.

In three exceptional samples of EscA, minimum values of less than 10% grain size > 20 μm occur. Two of these samples occur in e-marls (Fig. 6, peaks 1 and 5), and relate to minima of the carbonate content. The third sample, however, is situated in the middle of the couplet set and this thin bed does not appear in the outcrop as a dark layer (Fig. 5, peak 3; named M3(?)). Because of

the deviation from the characteristic grain size ranges of chalks, this peak would define the layer 'M3(?)' as a marl.

The percentage of grains $> 20 \mu\text{m}$ in marls is 20–40% in EscB (Fig. 7). A grain size minimum in a chalk was also identified (peak 4), which hints at the presence of a marly layer at this position as well (M4(?)). The overall higher grain size in marls of EscB compared to EscA is expressed by the less distinct outcrop appearance of marls higher up in the section. The grain size distribution of both EscA and EscB shows no clear relation to the c-dinocyst data and the gamma ray log.

3.2.3. Carbonate content and TOC

The carbonate content of EscA (Fig. 6) is positively related to the absolute abundances of the P-assemblage species and the Ps/Po-ratio. A gradual change can be recognised in the amplitude of

variation between marls and chalks (d_m in Fig. 6). The contrast is largest for the e-marls while in the middle of the bundle, the difference in carbonate content between marls and chalks is low. This trend is negatively related to the low-frequency curve in gamma ray values and the c-dinocyst data (Fig. 6) and also resembles the bundling of couplets in section EscA.

TOC values of the marls in EscA range from 0.15 to 0.26%, whereas those of the chalks range from 0.1 to 0.2%. There are no significant changes in carbonate content and TOC values between the marl types but, as with the carbonate content, the differences in TOC values between marls and chalks are largest in the couplets that contain the e-marls (Fig. 6).

In EscB (Fig. 7), the variations in carbonate content between marls and chalks is lower than in EscA (2–10%). Chalks have carbonate values as low as 85% while some marls show a maximum

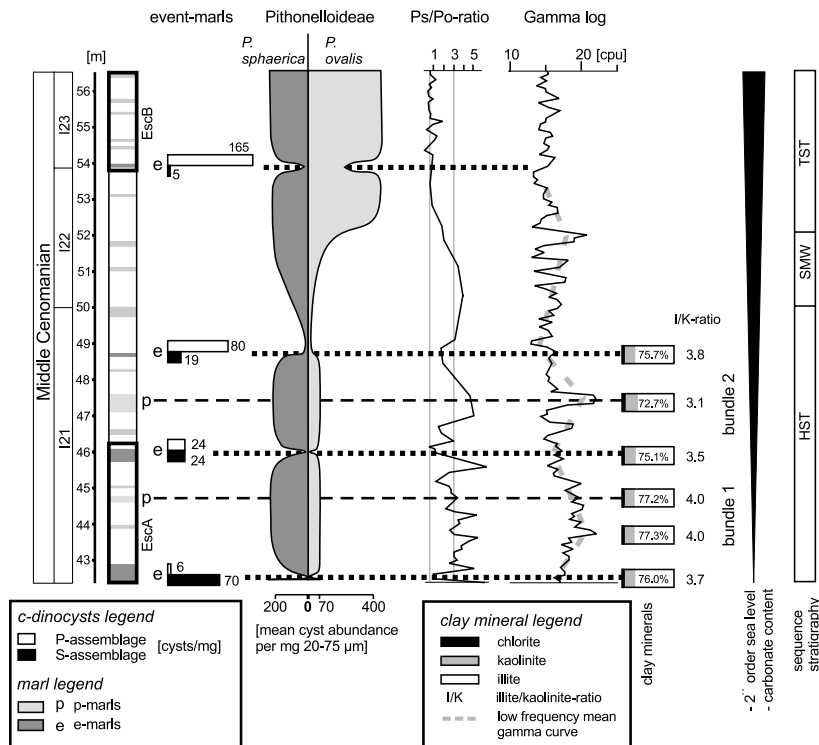


Fig. 9. Integrated illustration of the investigated section, showing trends in (i) e-marl characteristics; (ii) variations in mean *Pithonella sphaerica* and *P. ovalis* abundances and the Ps/Po-ratio; (iii) bundling of gamma ray log and clay mineral distribution; and (iv) sequence-stratigraphy after Robaszynski and Amédéo (1993): SMW = Shelf Margin Wedge, TST = Transgressive Systems Tract, HST = Highstand Systems Tract.

carbonate content of 88%. TOC values are between 0.15% and 0.32% in marls and range from 0.1% to 0.2% in the chalks.

3.3. Cycles between *EscA* and *EscB*, defined by the succession of marl types

An analysis of c-dinocysts of the interval from 46 m to 54 m between the section parts *EscA* and *EscB* was performed, with focus on the succession of the different marl types to test for continuous bundling (Fig. 9). The couplets following *EscA* can again be bundled into a set of five ('bundle 2' in Fig. 9). This bundle shows a comparable architecture to that of *EscA*, being bound by e-marls and gradually developing a p-marl in the middle of the succession (Fig. 9). Above this bundle, couplets cannot be bundled anymore by a systematic marl succession. The gamma ray signal and the lack of lows in mean absolute abundance of the P-assemblage suggest a relatively thick bundle of four couplets or a discontinuity in the succession (Fig. 9). The most important characteristic of this interval is the change which occurs in the Pithonelloideae assemblage. An increase of *P. ovalis* numbers between 52 m and 53 m leads to a significant shift of the mean Ps/Po-ratio from about 3 to 0.6.

4. Discussion

4.1. Transformation of the orbital-forcing signal into micropalaeontological cyclicity – bundling pattern and palaeoenvironmental interpretation

The mid-Cenomanian chalk–marl alternations of the Anglo–Paris Basin have been previously analysed by spectral analysis and the results support orbital forcing of the cycles (Gale et al., 1999). Here, an attempt is made to explain the transformation of the orbital signal into the sediment by interpreting the cyclic succession of different couplet types (defined here as marl types). The observed bundling of five chalk–marl couplets (Figs. 3, 6 and 9), strongly suggests the presence of a 5:1 modulation in amplitude of the precession signal by the 100-ka eccentricity cycle.

In *EscA*, the cyclicity is well reflected by the palaeontological and sedimentological parameters. Couplets containing e-marls show the most pronounced contrast in the investigated micropalaeontological parameters between chalk and marl (Figs. 3, 6 and 9). These couplets form the boundaries of the bundles. The observed amplification of couplets suggests increased low-frequency (eccentricity) modulation of the precession cycle. Thus, these bundle parts can be interpreted to have been deposited at eccentricity maxima. Contrary to these positions, interference of the usually negatively correlated abundances of the P-assemblage and the S-assemblage, the buffered positive and negative peaks of the Ps/Po-ratio around their mean value, and the small changes in TOC and carbonate content in the middle of the bundles (p-marls) all indicate a smaller contrast between the precession extremes during eccentricity minima. Since the bundling is well reflected by the c-dinocyst assemblages, we can attempt to palaeoecologically interpret the influence of the orbital variations on the palaeoenvironment.

Negatively related abundance trends of Pithonelloideae to the c-dinocysts contained in the S-assemblage have been observed by various authors in connection with sequence-scale sea level changes and water mass changes (Keupp, 1982, 1989, 1991; Zügel, 1994; Neumann, 1999). An invasion of *Pithonella ovalis* indeed occurs with the 3rd order transgression of sequence 4 and can be interpreted to indicate increased Tethyan influence towards the Upper Cenomanian (Fig. 9; chapter 4.3). The main character of the e-marls is the unusually high percentage of paratabulated forms (Fig. 3). Whereas Pithonelloideae are interpreted as being typical for the outer shelf (Bein and Reiss, 1976; Villain, 1981), the species of the S-assemblage were observed to be more abundant in marginal facies (Zügel, 1994). The distribution patterns in the marls (Fig. 9) would thus suggest a sea level fall during these episodes. However, it is unlikely that marginal facies zones expanded over the central areas of the Anglo–Paris Basin. It seems more plausible that the observed distribution pattern of c-dinocysts reflects oceanographic changes which are not primarily controlled by sea level fluctuations, but instead led to basin-wide

conditions typical of the marginal environment (e.g. a lagoonal or estuarine circulation). The paratabulated species discussed in the present study have been attributed to a group of Tethyan invaders into the Boreal Realm during transgressions in the Albian (Keupp, 1992; Neumann, 1999). They could therefore be interpreted to indicate surface water warming.

Pithonella sphaerica has been interpreted as an indicator of high carbonate production (Noel et al., 1995; Wendler et al., submitted), so that the very high Ps/Po-ratios in the chalks seem to indicate productivity peaks. In today's oceans, productivity of planktic organisms depends primarily on nutrient supply. Thus, a change from high to low abundance of calcareous primary producers in chalks and marls, respectively, may point to lower nutrient availability during marl formation with the most oligotrophic conditions prevailing during e-marl deposition.

Investigations on Recent calcareous dinoflagellates have shown that they are especially adapted to rather oligotrophic conditions and well stratified surface water masses (Höll et al., 1998; Vink, 2000). On the other hand, the highest diversity of c-dinocysts can be found in shelf areas where also stratified, but eutrophic conditions persist near the coast (Wall et al., 1977; Dale, 1983). An example is the Mediterranean Sea which has a highly diverse c-dinocyst association in both, oligotrophic and eutrophic environments (Montresor et al., 1998; and in the fossil record e.g.: Versteegh, 1993).

In conclusion, the significant changes in the investigated section between phases of low diversity/high numbers of specimens (chalks) and phases of high diversity/low numbers of specimens (e-marls) can be interpreted to reflect alternations between mixed and less circulated (possibly stratified) oceanographic conditions, respectively. Such oceanographic changes influence the supply of nutrients to the surface water environment. Oligotrophic conditions probably prevailed during times of greater stratification (e-marls), when transport of nutrients to the surface waters was hampered by stagnation. Low productivity during marl deposition in the investigated basin was also concluded from data on coccoliths (Young et al.,

1998) and foraminifera (Hart, 1980; Leary and Hart, 1992; Mitchell and Carr, 1998; Gräfe, 1999). The e-marls detected in the present study apparently reflect extremely low productivity, which was partly accompanied by selective dissolution at the water/sediment interface (especially of foraminifera) due to decreased accumulation rates of carbonate particles. The maximum abundances of *Heterohelix moremani* in the e-marls corroborate this interpretation of low productivity. This opportunist (Nederbragd et al., 1998) is known to have flourished during the uppermost Cenomanian oceanic anoxic event, when an extended oxygen minimum zone caused environmental stress on planktic life (Hart, 1996).

4.2. Transformation of the orbital-forcing signal into lithological cyclicity – gamma ray signature of the bundles

Governing the surface water carbonate productivity, precessional forcing passively influenced the quantity of non-carbonate in marls and chalks (Gräfe, 1999). This is reflected in the marls by a lower carbonate content, a smaller grain size and a higher gamma radiation compared to the chalks. However, although the carbonate content of the e-marls is low, they also have relatively low gamma ray values (Fig. 8). Additionally, the very low variation in carbonate content between the marl types cannot account for the differences in gamma ray values. Thus, an alternative explanation is needed for the low-frequency mean curve of the gamma ray, which reflects the bundling of couplets and thus seems to reflect the eccentricity cycle (higher gamma ray values during eccentricity minima compared to the eccentricity maxima; Figs. 6 and 9).

Bundling as is reflected in the low-frequency mean gamma ray curve (Fig. 9) is a prominent feature throughout the entire mid-Cenomanian (Fig. 5 in Gräfe, 1999). It could be interpreted on the basis of the clay minerals as (i) a change in the clay mineral association caused by climatic change; or (ii) a sea level change during the eccentricity cycle. Substantial climatic change causes qualitative variations in the association of clay minerals, especially the kaolonite:illite ratio (Mut-

terlose and Ruffell, 1999; Deconinck and Bernoulli, 1991; Deconinck et al., 1999). Kaolinite is the major clay mineral of erosion under the warm, humid conditions proposed for the Upper Cretaceous (Aróstegui et al., 1991; Deconinck and Chamley, 1995; Hallam et al., 1991; Thiry and Jacquin, 1993). It contains no radioactive elements. The most important clay mineral producing a gamma ray signal is illite. Illite-rich clay assemblages develop by erosion under rather dry conditions (Rösler, 1981; Singer, 1984). It could thus be postulated that more humid conditions under increased seasonality of the eccentricity maxima were replaced by a slightly drier climate during the eccentricity minima in the Anglo–Paris Basin. However, changes of the kaolinite/illite ratio in the clay mineral assemblage are also caused by sea level change (Singer, 1984; Van Buchem et al., 1992; Kunow et al., 1998). Kaolinite is deposited in the marginal facies whereas the smaller crystallites of illite are transported further into the basin. If a transgressive/regressive pattern had partly controlled the clay mineral association of the investigated cycles, then the increased gamma ray signal at the eccentricity minima would characterise these periods as regressive units.

The almost constant kaolinite/illite ratio between marls and chalks (Ditchfield, 1990), as well as between the e-marls and p-marls, suggests, however, that no significant climate change or sea level-controlled facies shift took place on the couplet (precession) and bundle (eccentricity) scale, respectively. Since changes in the clay association and TOC content are obviously insignificant, two factors that are related to productivity, the contribution of (i) phosphate (Glenn and Arthur, 1985; Wray, pers. com.) and (ii) the Sr/Ca ratio of the carbonate, could have influenced the low-frequency gamma ray mean curve. Due to the previously discussed relation between the bundling and surface water productivity, a plausible explanation for the gamma ray curve would be a higher phosphate content and/or an increased Sr/Ca ratio at the eccentricity minima, caused by an uninterrupted and high productivity. The addition of such a signal to the radiation caused by the clay minerals theoretically results in the observed low-frequency curve.

Besides clay minerals, organic matter and phosphate, other components of the marls and chalks may cause gamma radiation, such as, authigenic glaucony or radioactive detrital minerals. Future work on the mineralogy of the non-carbonate fraction is needed to completely solve the problem of the radiation sources.

4.3. Influence of the long-term sea level change on the transformation of the orbital-forcing signals

The long-term sea level trend seems to be critical for the preservation of the short-term orbital signals. The 100-ka eccentricity signals are more distinctly developed in the HST of sequence 3 (EscA) than in the TST of sequence 4 (EscB). Positioned in an interval of maximum sea level change, EscB is considered to represent a different, possibly less distinct or even incomplete succession due to fusing or erosion of individual couplets. The disturbed cyclicity above bundle 2 is related to the lowstand and subsequent transgression that have been reconstructed for this interval (Figs. 2 and 9). Niebuhr and Prokoph (1997) suggest that obscured symmetry in sedimentary successions is caused by chaotic sedimentation under the influence of transgression and lowstand conditions which overprints Milankovitch-related cyclicity. Poor preservation of the orbital signal within regressive units was also shown by Ricken (1994) in mid-Cretaceous cycles of the Western Interior Basin.

Besides disturbing the cyclical deposition, the long-term sea level change also appears to have influenced the distribution of Pithonelloideae in the investigated section. From 48.8 m to 52 m, the abundances of both *Pithonella sphaerica* and *P. ovalis* are significantly lower than in EscA, bundle 2 and EscB (Fig. 9). This interval is interpreted as the Shelf Margin Wedge (SMW) of sequence 3. Thus, the relative sea level lowstand is reflected by a Pithonelloideae minimum, indicating a basinward shift of their preferred facies zone which was the outer shelf. With the beginning of the *A. jukesbrownei* zone (TST of sequence 4), Pithonelloideae abundance increases considerably. The sea level-controlled increased overall abundance of *P. ovalis* would also explain the low rel-

ative abundance of the S-assemblage (3%) in the e-marl (M1 of EscB, Fig. 4). In addition to the influence of sea level change on the sedimentary preservation of orbitally forced signals, non-linear dynamics in the sedimentation have to be considered an important factor that may have obscured the reflection of the Milankovitch signal (Smith, 1994).

4.4. The palaeoenvironmental model

Simulation of Cretaceous climate shows that the largest effect of precession-controlled climate forcing is the modulation of the atmospheric (e.g. monsoonal) circulation (Park and Oglesby, 1990). Thus, the relation between orbital cycles, climate change and light/dark sedimentary cycles can be generally explained by two different mechanisms of wind-driven changes in sub-surface water circulation: (i) a monsoonal, salinity-driven model; and (ii) an anti-monsoonal, temperature-driven model (Herbert and Fischer, 1986).

Dark layers, which are organic-rich, can be thought to represent episodes of increased monsoonal intensity and enhanced atmospheric circulation in general, during which high terrigenous influx of freshwater and nutrients caused stratification (a freshwater surface layer) and very high bioproductivity, respectively (model (i)). This mechanism of eutrophication of the surface water is thought to have controlled, for example, the Pliocene/Pleistocene sapropel formation of the Mediterranean (e.g. Rossignol-Strick et al., 1982; Versteegh, 1994) and various Upper Cretaceous light/dark sedimentary cycles (e.g. Watkins, 1989; Boyd et al., 1994; Caron et al., 1999). As discussed in Sections 4.1 and 4.2, marls of the studied section represent periods of low productivity and constant terrigenous influx, so this model cannot be applied here. Mitchell and Carr (1998) combined sea level change with this eutrophication model. In their 'stratified water column model' for the Cenomanian of the Anglo-Paris Basin, they suggest that under peak oceanic influence, increased nutrient influx (supplied by flooding of shelf areas) led to high production which in turn caused oxygen depletion of the bottom waters. The problem with this mechanism is

that it applies oxygen depletion to force stratification, which is not possible. Oxygen depletion follows as a consequence of reduced circulation and stratification caused by density contrast between water layers.

Neither significant sea level changes nor varying terrestrial input by alternations between a humid and arid climate can be reconstructed in the present study. Therefore, we think that an anti-monsoonal mechanism, controlling basin circulation via wind stress instead of terrestrial run-off, caused the light/dark rhythmicity and its bundling (model (ii)). In this model, decreased energetic influence of wind systems, which at the investigated palaeogeographic position would be the Westerlies (e.g. Voigt, 1996), is considered to be the dominant factor controlling water column stratification. Thus, in an 'anti-monsoonal' model, deposition of dark layers took place during periods of low seasonal contrast, i.e. weakened atmospheric dynamics.

The energetic influence of the local wind system on the sea surface can control the circulation of a shelf basin in a coupled atmosphere–ocean system (Barron, 1983; Bottjer et al., 1986). Global temperature variation modifies the rate of precipitation (Barron et al., 1989) and the intensity of the wind systems in general. During times of high seasonality, wind systems such as the monsoon are stronger due to stronger pressure gradients between continents and oceans (De Boer and Smith, 1994). It is likely that the Cretaceous climate was generally characterised by intense mid-latitude depressions (Price et al., 1998) which would intensify the atmospheric circulation. Stronger winds lead to a more intense mixing of the surface waters, whereas low seasonality weakens this process. This can result in an intensely stratified upper water column during periods of low seasonality and reduced circulation in the basin. It is possible that saline, warm, oxygen-depleted, nutrient-poor surface water forms which can be subject to occasional downwelling if it becomes too dense. On a global scale, the latter is thought to have predominantly caused the production of warm, saline bottom water in low latitude shelf areas, leading to a deepening of the redoxcline that in turn caused the anoxic sedimen-

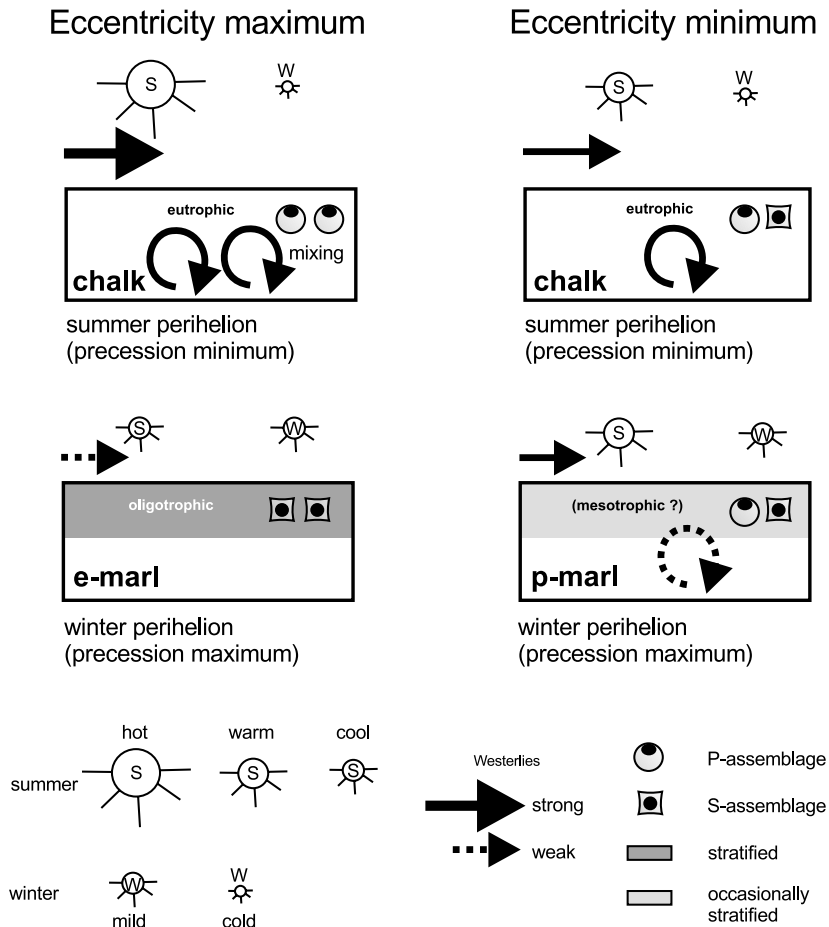


Fig. 10. Model of shelf basin circulation changes related to orbital forcing for the mid-Cenomanian of the Anglo-Paris Basin.

tation during the mid-Cretaceous (Brass et al., 1982; Bralower and Thierstein, 1984; Roth and Krumbach, 1986; Thierstein, 1989).

The relation between seasonality, the wind system, oceanic mixing and its influence on the c-dinocyst distribution is illustrated in Fig. 10. Orbital forcing amplifies seasonality in the northern hemisphere when our planet passes through perihelion during the northern summer. This situation is defined as the precession minimum (Berger, 1978; Hilgen et al., 1995; ten Veen and Postma, 1996). At this position, Earth receives the most summer insolation. During aphelion in the northern winter, when the irradiation angle is lowest, the Sun–Earth distance is highest and causes long, cold winters. In addition, the perihelion and ap-

helion distances are modified by the eccentricity cycle, which modulates the intensity of the seasonality. Consequently, lowest seasonality occurs during intervals of winter perihelion (precession maximum) and high eccentricity, which are the periods of e-marl deposition (i.e. the bundle boundaries). Well developed chalks, on the contrary, would represent peak seasonality at the summer perihelion, during which a well-mixed basin promoted high productivity. Organic matter was effectively recycled in the well-oxygenated water, leading to the deposition of a light, carbonate-rich limestone. In the eccentricity minima (for example the middle part of the bundle EscA), lithological changes are less distinct, and the c-dinocysts are very abundant in marls as well as in

chalks. Thus, we suggest that during times of decreased eccentricity with both summer and winter perihelion being less pronounced, i.e. without strong variations in seasonality, stratification occurred only temporarily and did not hamper bioproduction.

4.5. Double peaks – obliquity signal or negative biological feedback?

Several high-abundance peaks of *Pithonelloid* species appear as double peaks in the thickest chalks (i.e. peaks ‘A’ in EscA and ‘C’ and ‘D’ in EscB: Figs. 3 and 4). These double peaks may reflect (i) the additional influence of the obliquity cycle; or (ii) a negative ecological feedback to the precession minima. An expression of the obliquity cycle would be realistic, as this could well have buffered the precession signal (due to the modulation of insolation into an irregular sum-curve containing double peaks: see, for example, House, 1995), and could lead to the production of a ‘hidden marl’ within a chalk. Especially peak ‘C’ in EscB is related to a weak peak of paratabulated cysts, suggesting a short-term development of conditions typical for marl formation. It is striking that all three double peaks occur in exceptionally thick chalks, indeed suggesting that a ‘marl’ may be hidden. Theoretically, the obliquity signal could be present at the mid-latitudinal position of the section, but it was not found to be significant in time series analysis in the study area (e.g. Gale, 1999). In contrast, the Lower Cretaceous of the even more southward positioned Vocontian Basin is made up of carbonate cycles that are dominated by the obliquity cycle (Giraud et al., 1995). Thus, it is possible that a weak obliquity signal might be recorded in the investigated material.

The presence of a negative ecological feedback would be supported by the analysis of *Pithonella sphaerica* diameters in EscA (Fig. 3). The distinctive decrease in diameter at the double peak ‘A’ suggests environmental pressure, possibly due to competition with the other organisms that flourished during these episodes of generally enhanced bioproductivity. Thus, although the environmental conditions during the precession minima seem to have favoured productivity, a negative feed-

back in the size of *P. sphaerica* cysts can be observed which may indicate a decreased intensity of biomineralisation. Interestingly, a drop of mean as well as maximum test sizes in the middle of Cenomanian chalks has also been observed in benthic foraminifera (Leary and Hart, 1992). These authors assumed enhanced rates of gametogenesis or dwarfism due to an enhanced carbonate rain, i.e. ecological stress being the reason. No decrease in abundances was recorded for the benthic foraminifera. A temporary decrease of abundances of both benthic foraminifera and *Calcispheres* (= *Pithonelloideae*) in the middle of chalks of the Cenomanian from Folkstone/GB was also recorded by Ditchfield (1990). Although the double peaks may reflect an obliquity signal, the most straightforward explanation, because of the absence of size-decrease in the two analysed marls (M1 and M2 in EscA), is a negative biological feedback to enhanced productivity.

5. Conclusions

Precession-controlled light/dark couplets of the Middle Cenomanian show amplification and buffering by the superimposed eccentricity cycle.

1. Bundling of couplets can be recognised by *c-dinocyst* association changes that are in phase with variations in gamma ray and carbonate content. Bundles are defined by different marl types. The cyclicity in the micropalaeontological data clearly points to a palaeoecological origin of the signal.
2. Couplets showing strongest contrast in cyst association are interpreted as bundle boundaries that mark the eccentricity maxima, whereas weak couplets developed during eccentricity minima.
3. Orbitally forced climate change during the eccentricity cycle primarily controlled the basin circulation patterns but did not cause significant changes in terrestrial run-off or sea level.
4. The variations in oceanic circulation are reflected in the sediment by the chalk–marl couplets. Marls can be interpreted as the sedimentary expression of stratified surface water masses while chalks are representative of a well-mixed shelf sea

environment. Reduced oceanic mixing due to low seasonality during strong precession maxima at the eccentricity maxima caused periods of water column stratification that in turn led to nutrient depletion and decreased productivity in the surface water masses (e-marls). As a consequence, slightly increased surface temperatures in contrast to the well-mixed chalk episodes can be assumed.

Acknowledgements

A. Vink and I. Wendler are gratefully acknowledged for reviewing the final drafts of this manuscript. We thank C. Reichert and S. Bartsch for processing samples and performing LECO measurements. Valuable discussions with T. Bickert, A.S. Gale, S. Voigt, D. Wray and J.R. Young improved this investigation. This research was financially supported by the Deutsche Forschungsgemeinschaft, DFG-Project Wi 725/12.

Appendix. Taxonomy

The classification of calcareous dinoflagellate cysts is based on the four types of wall crystal orientation of these microfossils (Keupp and Mutterlose, 1984; Keupp, 1987; Janofske and Keupp, 1992). The four wall types of the Calciodinelloideae (Fensome et al., 1993) after Young et al. (1997) are: pithonelloid, oblique, radial and tangential.

Division:	DINOFLLAGELLATA (Bütschli, 1885) Fensome et al., 1993
Subdivision:	DINOKARYOTA Fensome et al., 1993
Class:	DINOPHYCEAE Pascher, 1914
Subclass:	PERIDINIPHYCIDAE Fensome et al., 1993
Order:	PERIDINIALES Haeckel, 1894
Family:	PERIDINIACEAE Ehrenberg, 1831
Subfamily:	CALCIODINELLOIDEAE Fensome et al., 1993

1. P-assemblage

Cenomanian assemblages of c-dinocysts are

dominated by Pithonelloideae, commonly called ‘calcispheres’. Pithonelloideae are double-walled cysts, each wall consisting of pithonelloid orientated calcite crystals (uniquely oblique, linear rows between apex and antapex on the cyst surface); (for detailed information on biomineralisation see Keupp and Kienel, 1994).

Genus

Pithonella Lorenz, 1902; emend. Bignot and Lezaud, 1964; emend. Villain, 1977 *Pithonella sphaerica* Kaufmann, 1865

Shape: Sphaerical cysts 20–120 µm diameter, cysts >70 µm rare; height/width ratio 0.9 to 1; mostly round archeopyles, 4–14 µm diameter; a row of crystals occasionally surrounds the opening.

Stratigraphic range: Upper Barremian (Keupp, 1987) to Lower Danian? (Kienel, 1994).

Pithonella ovalis Kaufmann, 1865

Shape: Ovoid, apically–antapically elongated form of the genus *Pithonella*.

Stratigraphic range: as *P. sphaerica*

Pithonella discoidea Willems, 1992

Shape: Disc-shaped; apical–antapically flattened cysts of the genus *Pithonella* with a height/width ratio below 0.5 and an equatorially running suture line (similar to *Normandia circumperforata* Zügel, 1994); 29–70 µm in equatorial diameter.

Stratigraphic range: mid-Cenomanian to Maastriichtian (range extended from originally only Maastriichtian to the mid-Cenomanian due to the findings of the present study).

The following species are characterised by a cyst wall with an oblique crystal orientation. The most abundant species are *Cubodinellum renei* and *Pentadinellum vimineum*, which show a reduced paratabulation. Having a wide lateral and stratigraphical range and specific ecological demands, they are not of biostratigraphic value but are very suitable for the study of cyclical environmental changes. Due to their distinctive paratabulation, they are easy to determine with the binocular microscope and used for countings

without extensive SEM-studies being necessary.

Genus *Pirumella* Bolli, 1980

The most abundant oblique spherical cysts in the studied material all belong to the same species whose exact affinity is not unequivocally determinable. The two possibilities are: (i) *Pirumella carteri* Bolli, 1974; or (ii) remains of double-walled cysts (*Pirumella multistrata* group) with the outer wall having been mechanically removed (as described by Keupp, 1989).

Shape: 29–55 µm in diameter, most likely with oblique wall crystal orientation. Only one thin wall is present. Surface crystals are lath-shaped and obliquely oriented. Appearance in the light microscope: transparent, slightly reflective surface in contrast to *Pithonella* spp. The archeopyle diameter varies from 7 to 15 µm, commonly about of the cyst diameter. The archeopyle is often elongated or slightly 8-shaped and frequently has an elevated rim.

Rare species:

Normandia circumperforata Zügel, 1994

Pithonella cardiiformis Zügel, 1994

2. S-assemblage

Cubodinellum renei Keupp, 1987

Shape: 20–35 µm in size, showing a paratabulation pattern giving it a cubic shape. The paratabulation is formed by perpendicular edges of coarser crystals on a spherical inner cyst body. The single wall consists of thin, needle-shaped, obliquely orientated crystals.

Stratigraphic range: mid-Albian to Late Cenomanian.

Pentadinellum(?) vimineum Keupp, 1987

Shape: Carinate, hat-shaped cyst; paratabulation consists of an occasionally asymmetric pentagonal cingular ridge, 20–53 µm in diameter. This ridge is attached to a spherical inner cyst body, 15–22 µm in diameter. The archaeopyle is

7.4–17 µm in diameter. The single wall consists of thin, needle-shaped, obliquely orientated crystals.

Stratigraphic range: mid-Albian to Maastrichtian (Wendler and Willems, submitted)

Rare species:

(oblique wall type)

Gonellum kurti Keupp, 1987

Pirumella labyrinthica Zügel, 1994

Pirumella cf. *porosa* (Pflaumann and Krashennikov, 1978)

Pirumella scobidota Zügel, 1994

Saumuria sp. Zügel, 1994

(radial wall type)

Orthopithonella cf. *gustafsoni* Bolli, 1974

References

- Aróstegui, J., Zuluaga, M.C., Velasco, F., Ortega-Huertas, M., Nieto, F., 1991. Diagenesis of the central Basque–Cantabrian Basin (Iberian peninsula) based on illite–smectite distribution. *Clay Miner.* 26 (4), 535–548.
- Barron, E.J., 1983. A warm and equable Cretaceous: the nature of the problem. *Earth Sci. Rev.* 19, 305–338.
- Barron, E.J., Hay, W.W., Thompson, S.L., 1989. The hydrologic cycle: a major variable during Earth history. *Palaeogeogr. Palaeoclimatol. Palaeoecol.* 75, 157–174.
- Bein, A., Reiss, Z., 1976. Cretaceous Pithonella from Israel. *Micropaleontology* 22, 83–91.
- Berger, A.L., 1978. Long-term variations of daily insolation and Quaternary climatic cycles. *J. Atmos. Sci.* 35, 2362–2367.
- Bignot, G., Lezaud, L., 1964. Contribution à l'étude des *Pithonella* de la craie parisienne. *Rev. Micropaléontol.* 7, 138–152.
- Bottjer, D.J., Arthur, M.A., Dean, W.E., Hattin, D.E., Savrda, C.E., 1986. Rhythmic bedding produced in Cretaceous pelagic carbonate environments: sensitive recorders of climatic cycles. *Paleoceanography* 1 (4), 467–481.
- Bouyx, E., Villain, J.-M., 1986. Microfaunes et microfacies du Crétacé Supérieur de l'extrémité occidentale de l'Hindou Kouch (Afghanistan). *Cretac. Res.* 7, 327–347.
- Boyd, R., Huang, Z., O'Connell, S., 1994. Milankovitch cyclicity in late Cretaceous sediments from Exmouth Plateau off Northwest Australia. *Spec. Publ. Int. Assoc. Sedimentol.* 19, 145–166.
- Bralower, T.J., Thierstein, H.R., 1984. Low productivity and slow deep-water circulation in mid-Cretaceous oceans. *Geology* 12, 614–618.
- Brass, G.W., Southam, J.R., Peterson, W.H., 1982. Warm saline bottom waters in the ancient ocean. *Nature* 296, 620–623.
- Caron, M., Robaszynski, F., Amedro, F., Baudin, F., Decoininck, J.-F., Hochuli, P., von Salis-Perch Nielsen, K., Tribouillard, N., 1999. Estimation de la durée de l'événement anoxique global au passage Cénoman/Turonien. Approche

- cyclostratigraphique dans la formation Bahloul en Tunisie centrale. *Bull. Soc. Géol. Fr.* 2, 145–160.
- Dale, B., 1983. Dinoflagellate resting cysts: benthic plankton'. In: Fryxell, G.A. (Ed.), *Survival strategies of the Algae*. Cambridge University Press, Cambridge, pp. 69–136.
- Dali-Ressot, M.-D., 1987. Les Calcisphaerulidae des terrains Albien à Maastrichtien de Tunisie centrale (J. Bireno et J. Bou el Ahneche): intérêts systématique, stratigraphique et paléogéographique. PhD thesis, University Tunis, Unpublished, 191 pp.
- De Boer, P.L., Smith, D.G., 1994. Orbital forcing and cyclic sequences. *Spec. Publ. Int. Assoc. Sedimentol.* 19, 1–14.
- Deconinck, J.-F., Bernoulli, D., 1991. Clay mineral assemblages of Mesozoic pelagic and flysch sediments of the Lombardian Basin (Southern Alps): implications for palaeotectonics palaeoclimate and diagenesis. *Geol. Rundsch.* 80 (1), 1–17.
- Deconinck, J.-F., Chamley, H., 1995. Diversity of smectite origins in late Cretaceous sediments: example of chalks from northern France. *Clay Miner.* 30, 365–379.
- Deconinck, J.-F., Vanderaverot, P., Amedro, F., Collete, C., Robaszynski, F., 1999. Origin of clay minerals in Cenomanian and Turonian chalks from northern France: a review. 19th Regional European Meeting of Sedimentology Abstracts, 69.
- Dias-Brito, D., 2000. Global stratigraphy, palaeobiogeography and palaeoecology of Albian–Maastrichtian pithonellid calcispheres: impact on Tethys configuration. *Cretac. Res.* 21, 315–349.
- Ditchfield, P.W., 1990. Milankovitch cycles in Cenomanian chalks of the Anglo–Paris Basin. PhD thesis, University of Liverpool, Liverpool, Unpublished, 200 pp.
- Fensome, R.A., Taylor, F.J. R., Norris, G., Sarjeant, W.A. S., Wharton, D.I., Williams, G.L., 1993. A classification of living and fossil dinoflagellates. *Micropalaeontol., Spec. Publ.* 7, 351 pp.
- Fischer, A.G., Schwarzacher, W., 1984. Cretaceous bedding rhythms under orbital control? In: Berger, A.L., Imbrie, J., Hays, J., Kukla, G., Saltzman, B. (Eds.), *Milankovitch and climate, Part 1*. D. Reidel Publishing Company, Dordrecht, 1984, pp. 163–175.
- Gale, A.S., 1990. A Milankovitch scale for Cenomanian time. *Terra Nova* 1, 420–425.
- Gale, A.S., 1995. Cyclostratigraphy and correlation of the Cenomanian Stage in western Europe. In: House, M.R. and Gale, A.S. (Eds.), *Orbital forcing, timescales and cyclostratigraphy*. *Geol. Soc. Lond., Spec. Publ.* 85, 177–197.
- Gale, A.S., Young, J.R., Shackleton, N.J., Crowhurst, S.J., Wray, D.S., 1999. Orbital tuning of Cenomanian marly chalk successions: towards a Milankovitch time-scale for the late Cretaceous. *Phil. Trans. R. Soc. Lond. A* 357, 1815–1829.
- Giraud, F., Beaufort, L., Cotillon, P., 1995. Contrôle astronomique de la sédimentation carbonatée dans le Crétacé inférieur du Bassin Vocontien (SE France). *Bull. Soc. Géol. Fr.* 166 (4), 409–421.
- Glenn, C.R., Arthur, M.A., 1985. Sedimentary and geochemical indicators of productivity and oxygen contents in modern and ancient basins: The Holocene Black Sea as the 'type' anoxic basin. *Chem. Geol.* 48, 325–354.
- Gräfe, K.-U., 1999. Foraminiferal evidence for Cenomanian sequence stratigraphy and palaeoceanography of the Boulonnais (Paris Basin, northern France). *Palaeogeogr. Palaeoclimatol. Palaeoecol.* 153, 41–70.
- Hallam, A., Grose, J.A., Ruffell, A.H., 1991. Palaeoclimatic significance of changes in clay mineralogy across the Jurassic–Cretaceous boundary in England and France. *Palaeogeogr. Palaeoclimatol. Palaeoecol.* 81, 173–187.
- Haq, B.U., Hardenbol, J., Vail, P.R., 1987. Chronology of fluctuating sea level since the Triassic. *Science* 235, 1156–1166.
- Hart, M.B., 1980. The recognition of mid-Cretaceous sea level changes by means of foraminifera. *Cretac. Res.* 1, 289–297.
- Hart, M.B., 1996. Recovery of the food chain after the late Cenomanian extinction event. In: Hart, M.B. (Ed.), *Biotic recovery from mass extinction events*. *Geol. Soc. Lond., Spec. Publ.* 102, 265–277.
- Herbert, T.D., Fischer, A.G., 1986. Milankovitch climatic origin of mid-Cretaceous black shale rhythms in central Italy. *Nature* 321 (19), 739–743.
- Hilgen, F.J., Krijgsman, W., Langereis, C.G., Lourens, L.J., Santarelli, A., Zachariasse, W.J., 1995. Extending the astronomical (polarity) time scale into the Miocene. *Earth and Planet. Sci. Lett.* 136, 495–510.
- Höll, C., Zonneveld, K.A.F., Willems, H., 1998. On the ecology of calcareous dinoflagellates: The Quaternary Eastern Equatorial Atlantic. *Mar. Micropaleontol.* 33, 1–25.
- House, M.R., 1995. Orbital forcing timescales: an introduction. In: House, M.R., Gale, A.S. (Eds.), *Orbital forcing, timescales and cyclostratigraphy*, *Geol. Soc. Lond., Spec. Publ.* 85, 1–18.
- Kaufmann, F.J., 1865. Polythalamien des Seewerkalkes. In: Heer, O. (Ed.), *Die Urwelt der Schweiz*, pp. 194–199.
- Kennedy, W.J., 1967. Burrows and surface traces from the Lower Chalk of southern England. *Bull. Br. Mus. Nat. Hist. Geol.* 15, 127–167.
- Keupp, H., 1982. Die kalkigen Dinoflagellaten-Zysten des späten Apt und frühen Alb in Nordwestdeutschland. *Geol. Jahrb. A* 65, 307–363.
- Keupp, H., 1987. Die kalkigen Dinoflagellaten-Zysten des Mittelalb bis Untercenoman von Escalles/Boulonnais (N-Frankreich). *Facies* 16, 37–88.
- Keupp, H., Ilg, A., 1989. Die kalkigen Dinoflagellaten im Ober-Callovium und Oxfordium der Normandie/Frankreich. *Berl. Geowiss. Abh. A* 106, 165–205.
- Keupp, H., 1991. Kalkige Dinoflagellatenzysten aus dem Eibrunner Mergel (Cenoman-Turon-Grenzbereich) bei Abbach/Süddeutschland. *Berl. Geowiss. Abh. A* 134, 127–145.
- Keupp, H., 1992. Die Flora kalkiger Dinoflagellaten-Zysten im mittleren Alb (Gargas) der Kernbohrung Himstedt 3 bei Hoheneggelsen/Niedersachsen. *Berl. Geowiss. Abh. E* 3, 121–169.
- Keupp, H., 1993. Kalkige Dinoflagellaten-Zysten in Hell-Dunkel-Rhythmen des Ober-Hauterive/Unter-Barrême NW-Deutschlands. *Zitteliana (Hagn/Herm-Festschrift)* 20, 25–39.

- Keupp, H., Kienel, U., 1994. Wandstrukturen bei Pithonelloideae (Kalkige Dinoflagellaten-Zysten): Biomineralisation und systematische Konsequenzen. *Abh. Geol. A* 50, 197–217.
- Keupp, H., Mutterlose, J., 1984. Organismenverteilung in den D-Beds von Speeton (Unterkreide, England) unter besonderer Berücksichtigung der kalkigen Dinoflagellaten-Zysten. *Facies* 10, 153–178.
- Kienel, U., 1994. Die Entwicklung der kalkigen Nannofossilien und der kalkigen Dinoflagellaten-Zysten an der Kreide/Tertiär-Grenze in Westbrandenburg im Vergleich mit Profilen in Nordjütland und Seeland (Dänemark). *Berl. Geowiss. Abh. E* 12, 87 pp.
- Kunow, R., Bauer, J., Bachmann, M., Kuss, J., 1998. Verteilungsmuster benthischer Foraminiferen und Tonmineralassoziationen im Oberapt des Sinai. english title: Distribution patterns of benthic foraminifera and clay mineral associations of Late Aptian sediments, Sinai. *Zbl. Geol. Paläontol.* 1 (12), 353–371.
- Leary, P.N., Hart, M.B., 1992. The benthonic foraminiferal response to changing substrate in Cenomanian rhythms induced by orbitally-forced surface water productivity. *J. Micropalaeontol.* 11 (2), 107–111.
- Mitchell, S.F., Carr, I.T., 1998. Foraminiferal response to mid-Cenomanian (Upper Cretaceous) palaeoceanographic events in the Anglo-Paris Basin (Northwest Europe). *Palaeogeogr. Palaeoclimatol. Palaeoecol.* 137, 103–125.
- Montresor, M., Zingone, A., Sarno, D., 1998. Dinoflagellate cyst production at a coastal Mediterranean site. *J. Plankton Res.* 20 (12), 2291–2312.
- Mutterlose, J., 1989. Faunal and floral distribution in late Hauterivian rhythmic bedded sequences and their implications. In: Wiedmann, J. (Ed.), *Cretaceous of the western Tethys. Proceedings of the 3rd International Cretaceous Symposium*, Tübingen, 1987. Schweizerbart, Stuttgart, pp. 691–713.
- Mutterlose, J., Ruffell, A., 1999. Milankovitch-scale palaeoclimate changes in pale-dark bedding rhythms from the early Cretaceous (Hauterivian and Barremian) of eastern England and northern Germany. *Palaeogeogr. Palaeoclimatol. Palaeoecol.* 154, 133–160.
- Nederbragd, A.J., Erlich, R.N., Fouke, B.W., Ganssen, G.M., 1998. Palaeoecology of the biserial planktonic foraminifer *Heterohelix moremani* (Cushman) in the late Albian to middle Turonian Circum-North Atlantic. *Palaeogeogr. Palaeoclimatol. Palaeoecol.* 144, 115–133.
- Neumann, C., 1999. Diversitäts- und Häufigkeitsmuster kalkiger Dinoflagellatenzysten aus dem Alb (Unterkreide) der Bohrung Kirchrode II (Niedersächsisches Becken, NW-Deutschland) und ihre möglichen Steuerungsmechanismen. *Berliner Geowiss. Abh. E* 31, 79 pp.
- Niebuhr, B., Prokoph, A., 1997. Periodic cyclic and caotic successions of Upper Cretaceous (Cenomanian to Campanian) pelagic sediments in the North German Basin. *Cretac. Res.* 18, 731–750.
- Noel, D., Busson, G., Mangin, A.-M., Cornée, A., 1995. La Distribution des Pithonelles dans le Cénomanien inférieur et moyen du Boulonnais (Nord de la France): Liaison avec les alternances craies/craies marseuses et implications environnementales et historiques. *Rev. Micropaléontol.* 38 (3), 245–255.
- Obradovich, J., 1994. Cretaceous time scale. In: Caldwell, W.G.E., Kauffman, E.G. (Eds.), *Evolution of the Western Interior Basin*. Geological Association of Canada, Spec. Pap. 39, pp. 379–396.
- Owen, D., 1996. Interbasinal correlation of the Cenomanian stage; testing the lateral continuity of sequence boundaries. In: Howell, J.A., Aitken, J.F. (Eds.), *High resolution sequence stratigraphy: Innovations and applications*. Geol. Soc. Lond., Spec. Publ. 104, 269–293.
- Park, J., Ogllesby, R.J., 1990. A comparison of precession and obliquity effects in a Cretaceous paleoclimate simulation. *Geophys. Res. Lett.* 17, 1929–1932.
- Price, G.D., Valdes, P.J., Sellwood, B.W., 1998. A comparison of GCM simulated Cretaceous 'greenhouse' and 'icehouse' climates: implications for the sedimentary record. *Palaeogeogr. Palaeoclimatol. Palaeoecol.* 142, 123–138.
- R.O.C.C. (Research on Cretaceous Cycles) Group., 1986. Rhythmic bedding in Upper Cretaceous pelagic carbonate sequences Varying sedimentary response to climatic forcing. *Geology* 14, 153–156.
- Ricken, W., 1986. Diagenetic bedding. *Lect. Notes Earth Sci.* 6, 1–209.
- Ricken, W., 1994. Complex rhythmic sedimentation related to third-order sea-level variations: Upper Cretaceous, Western Interior Basin, USA. *Spec. Publ. Int. Assoc. Sedimentol.* 19, 167–193.
- Robaszynski, F., Amédéo, F., 1993. Les falaises crétacées du Boulonnais. La coupe de référence du Cap Blanc-Nez dans un contexte sédimentaire global. *Ann. Soc. Géol. Nord* 2, 31–44.
- Robaszynski, F., Juignet, P., Gale, A.S., Amédéo, F., Hardenbol, J., 1998. Sequence stratigraphy in the Upper Cretaceous series of the Anglo-Paris Basin: exemplified by the Cenomanian stage. In: De Graciansky, P.C., Hardenbol, J., Jacquini, T., Vail, P.R., Farley, M.B. (Eds.), *Mesozoic-Cenozoic sequence stratigraphy of European basins*. Soc. Econ. Paleontol. Mineral. Spec. Publ. 60, 363–386.
- Rösler, H.J., 1981. *Lehrbuch der Mineralogie*. VEB Deutscher Verlag für Grundstoffindustrie, Leipzig, 834 pp.
- Rosignol-Strick, M., Nesteroff, W., Olive, P., Vergnaud-Grazzini, C., 1982. After the deluge; Mediterranean stagnation and sapropel formation. *Nature* 295, 105–110.
- Roth, P.H., Krumbach, K.R., 1986. Middle Cretaceous calcareous nannofossil biogeography and preservation in the Atlantic and Indian Oceans: Implications for paleoceanography. *Mar. Micropaleontol.* 10, 235–266.
- Schwarzacher, W., 1993. Cyclostratigraphy and the Milankovitch theory. *Dev. Sedimentol.* 52, 225.
- Schwarzacher, W., 1994. Cyclostratigraphy of the Cenomanian in the Gubbio district, Italy: a field study. *Spec. Publ. Int. Assoc. Sedimentol.* 19, 87–97.
- Singer, A., 1984. The paleoclimatic interpretation of of clay minerals in sediments – a review. *Earth Sci. Rev.* 21, 251–293.

- Smith, D.G., 1994. Cyclicity or chaos? Orbital forcing versus non-linear dynamics. Spec. Publ. Int. Assoc. Sedimentol. 19, 531–544.
- Ten Veen, J.H., Postma, G., 1996. Astronomically forced variations in gamma-ray intensity: Late Miocene hemipelagic successions in the eastern Mediterranean Basin as a test case. *Geology* 24 (1), 15–18.
- Thierstein, H.R., 1989. Inventory of palaeoproductivity records: The mid-Cretaceous enigma. In: Berger, W.H., Smetacek, V.S., Wefer, G. (Eds.), *Productivity of the Oceans: Present and Past*, pp. 355–375.
- Thiry, M., Jacquin, T., 1993. Clay mineral distribution related to rift activity, sea-level changes and paleoceanography in the Cretaceous of the Atlantic Ocean. *Clay Miner.* 28, 61–84.
- Van Buchem, F.S.P., Melnyk, D.H., McCave, I.N., 1992. Chemical cyclicity and correlation of Lower Lias mudstones using gamma ray logs, Yorkshire, UK. *J. Geol. Soc. Lond.* 149, 991–1002.
- Versteegh, G.J.M., 1993. New Pliocene and Pleistocene calcareous dinoflagellate cysts from southern Italy and Crete. *Rev. Palaeobot. Palynol.* 78, 353–380.
- Versteegh, G.J.M., 1994. Recognition of cyclic and non-cyclic environmental changes in the Mediterranean Pliocene. *Mar. Micropaleontol.* 23, 141–171.
- Villain, J.-M., 1975. 'Calcisphaerulidae' (*incertae sedis*) du Crétacé supérieur du Limbourg (Pays-Bas) et d'autres régions. *Palaeontogr. A* 149, 193–242.
- Villain, J.-M., 1981. Les Calcisphaerulidae: intérêt stratigraphique et paléocéologique. *Cretac. Res.* 2, 435–438.
- Vink, A., 2000. Reconstruction of Recent and Late Quaternary surface water masses of the western Subtropical Atlantic Ocean based on calcareous and organic-walled dinoflagellate cysts. *Ber. Fachber. Geowiss. Universität Bremen* 159, 160 pp.
- Voigt, S., 1996. Paläobiogeographie oberkretazischer Inoceramen und klimatologische Konsequenzen einer neuen Paläogeographie. *Münch. Geowiss. Abh. (A) Geol. Paläontol.* 31, 5–102.
- Wall, D., Dale, B., Lohmann, G.P., Smith, W.K., 1977. The environmental and climatic distribution of dinoflagellate cysts in modern marine sediments from regions in the north and south Atlantic Ocean and adjacent seas. *Mar. Micropaleontol.* 2, 121–200.
- Watkins, D.K., 1989. Nannoplankton productivity fluctuations and rhythmically-bedded pelagic carbonates of the Greenhorn Limestone (Upper Cretaceous). *Palaeogeogr. Palaeoclimatol. Palaeoecol.* 74, 75–86.
- Wendler, J., Gräfe, K.-U., Willems, H., submitted. Palaeoecology of calcareous dinoflagellate cysts in the mid-Cenomanian Boreal Realm – implications for the reconstruction of palaeoceanography of the NW European shelf sea. *Cretaceous Res.*
- Willems, H., 1992. Kalk-Dinoflagellaten aus dem Unter-Maastricht der Insel Rügen. *Z. Geol. Wiss.* 20 (1/2), 155–178.
- Young, J.R., Bergen, J.A., Bown, P.R., Burnett, J.A., Fiorentino, A., Jordan, R.W., Kleijne, A., van Niel, B.E., Romein, A.J.T., von Salis, K., 1997. Guidelines for coccolith and calcareous nannofossil terminology. *Palaeontology* 40, 875–912.
- Young, J.R., Gale, A.S., Tazzi, M., Brown, P.R., Windley, D., 1998. Cenomanian nannofossils and Milankovitch cyclicity. Abstracts of the 7th Conference of the International Nannoplankton Association, Puerto Rico.
- Ziegler, W.H., 1975. Outline of the geological history of the North Sea. *Geology* 1, 165–190.
- Ziegler, P.A., 1990. Geological atlas of western and central Europe. Shell Int. Petrol. Maatsch., The Hague.
- Zügel, P., 1994. Verbreitung kalkiger Dinoflagellaten-Zysten im Cenoman/Turon von Westfrankreich und Norddeutschland. *Cour. Forsch.-Inst. Senckenb.* 176, Frankfurt a.M., pp. 1–159.